Desalination and Water Treatment
www.deswater.com

doi: 10.5004/dwt.2022.28581

257 (2022) 158–168
May

Olive oil mill wastewater treatment by a combined process of freezing, sweating and thawing

Youness El Haimer, Anouar Rich*, Mhammed Sisouane, Mostapha Siniti, Mohammed El Krati, Soufiane Tahiri, Mohammed Mountadar

Laboratoryof Water and Environment, Department of Chemistry, Faculty of Sciences, Chouaïb Doukkali University, El Jadida, Morocco, Tel. +212 6 66 31 90 93; emails: rich.anouar7@gmail.com (A. Rich), younesselhaimer@gmail.com (Y. El Haimer), mhammed.sisouane@gmail.com (M. Sisouane), msiniti@yahoo.fr (M. Siniti), elkrati1@yahoo.fr (M. El Krati), tahiri.s@ucd.ac.ma (S. Tahiri), mounta_dar@yahoo.fr (M. Mountadar)

Received 31 January 2022; Accepted 23 May 2022

ABSTRACT

The aim of this work is the treatment of olive oil mill wastewater (OMW) by a combined process based on freezing, sweating and thawing. The process consists of two main steps: (i) cooling and freezing at –24°C, and (ii) sweating or fractional melting of ice at room temperature. Five liquid fractions (F_1, F_2, F_3, F_4 and F_5) were recovered and analyzed. The effectiveness of treatment was evaluated based on physico-chemical parameters such as pH, conductivity, dry matter, organic matter (OM), total phenols, chemical oxygen demand (COD), mineral matter (MM) and elemental mineral composition. UV-Visible and Fourier-transform infrared spectroscopy were also applied for this purpose. Results show that OMW effluent has an acidic pH and is loaded with OM and MM. The best operating conditions for treating OMW by block freezing have been highlighted. The concentration index (CI) of the first cryoconcentrated liquid fraction (F_1) is about 3.6 and 1.5 for OM and MM, respectively. This fraction is the most concentrated in phenolic compounds (100.2 g/L). The second cryoconcentrated liquid fraction (F_2) has a CI of about 1.7 and 0.6 for OM and MM, respectively. The CI corresponding to F_3 liquid fraction is around 1.2 and 0.5 for OM and MM, respectively. This liquid has physico-chemical characteristics similar to those of raw OMW. The CI corresponding to F_4 liquid fraction decreased to values 0.65 and 0.25 for the same parameters (OM and MM), respectively. The analysis of F_5 fraction shows that sweating step allows a thorough purification of ice block. The CI corresponding to F_5 is about 0.35 for OM, it reflects well COD and total phenols concentrations analyzed. The CI for MM was also significantly reduced to reach a value of 0.12 which is in agreement with potassium, phosphate, calcium, sulfur, magnesium and sodium concentrations. In general, the results demonstrate the feasibility of the suggested process and give a good idea of the operating conditions that can be employed to cryoconcentrated phenolic compounds in OMW for a possible industrial application.

Keywords: Treatment; Olive oil mill wastewater; Block freeze concentration; Cryoconcentration; Phenolic compounds

1. Introduction

The cultivation of olive trees is part of the Mediterranean tradition. According to the International Olive Council, the Mediterranean region provides 97% of the total world olive production. The olive oil extraction generates two by-products which are the olive pomace and olive-vegetation water called olive oil mill wastewater (OMW). Due to their high organic loads, and high amounts of organic acids and phenolic compounds [1,2], OMW are toxic for ecosystem and

* Corresponding author.

Presented at the Second International Symposium on Nanomaterials and Membrane Science for Water, Energy and Environment (SNMS-2021), June 1–2, 2022, Tangier, Morocco

are considered one of the most harmful effluents produced by the food industry. It was estimated that OMW are 200-400 times more toxic than municipal wastewater [3]. Thus, the treatment of these effluents is a major challenge for Mediterranean countries.

Many ways of detoxification, treatment, or recovery of OMW are being explored to make OMW less toxic or easier to process. These effluents are used as a possible dye bath for dyeing wool [4], a source of antifungal agents [5], a liquid affecting the soil microbial communities [6], a waste for biogas production after ultrasound pretreatment [7], a matter for co-composting with solid OMW [8], an antioxidants [9], etc. The treatment of OMW by physical, chemical and biological methods has been the subject of several research works. Their main objective is to study and propose the best technologies for minimizing environmental impacts, and for optimizing the treatment and recovery of OMW [10-18].

Concentration techniques are widely used as a preparation step in the food industry before drying in order to produce concentrated foods and solutions of different categories. Currently, there are four concentration techniques, including vacuum evaporation, reverse osmosis and to a lesser extent, concentration by freezing (cryoconcentration) and freeze drying.

Several studies have shown that evaporation requires a large amount of energy due to the high latent heat of water vaporization. The evaporation technique is not suitable for solutions containing volatile organic compounds as it may promote the formation of some hazardous gases [19]. The factors that can affect the evaporation process are fouling and maximum viscosity at the outlet of the evaporator [20].

In the case of reverse osmosis, the elimination of water is carried out through a dense membrane. This method requires little energy compared to evaporation because there is no phase change. However, the membrane used in the process is always subject to clogging and fouling, which can later lead to a reduction in the life of the membrane. This could result in a high cost not only for maintenance and replacement of the membrane, but also to achieve the osmotic pressure, which is required for the process [21,22].

Research carried out on the economic evaluation of the cold-wall freezing desalination process indicates that the energy consumption of a small installation could be very low. Indeed, the study has shown that freezing is positioned between reverse osmosis, less greedy (between 3 and 5 kWh/m^3) and distillation (24-27 kWh/m^3). Calculations show that the energy consumption of desalination by freezing is approximately 10 kWh/m^3 [23,24]. Recent work Melak et al. [25] indicates that the coupling between reverse osmosis and freezing can reduce energy consumption to 5.17 kWh/m^3.

The crystallization treatment is used in several fields such as desalination and industrial water treatment. It consists in cryoconcentrating (freezing) the solution. It has many advantages [26]: clean, ecological (no organic solvents, no chemical additives), and less energy consuming than the thermal process. The technique also allows preserving the quality of the compounds to be recovered. At one level, it enables their separation, concentration, and recovery [27]. The freezing treatment process needs approximately 1/7th of the latent heat required by the vaporization-based desalination processes. The involvement of sub-zero temperature in freezing treatment reduces the risk of corrosion and scaling. At another level, it permits the production of clean water. This approach reduces discharges and produces purified water for various uses. The technique also makes it possible to reduce the volume of stored quantities.

Freezing techniques are classified into three main categories: block freezing, suspension freezing, and cold wall freezing. First, the block freezing concentration technique has been developed for the treatment of industrial waters containing sulfuric acid [28] and of seawater desalination [23–25,29–34]. The technique has been developed for food products such as the concentration of milk solutions [35] and the concentration of orange juice [36]. Second, the suspension freezing concentration technique was applied for the treatment of cationic resin regeneration water [37]. Finally, cold wall freezing was developed for industrial wastewater treatment [38].

The present study aims at developing a treatment process of OMW based on cryoconcentration in order to obtain concentrated solutions rich in phenolic compounds. The process consists of two main steps: (i) the cooling and freezing at –24°C, and then (ii) the sweating step or fractional melting of the ice at room temperature. The effectiveness of the treatment was evaluated by determining the physico-chemical parameters of the cryoconcentrated liquid fractions and by using UV-Visible and Fourier-transform infrared spectroscopy (FTIR).

2. Materials and methods

2.1. Sampling of OMW

Sampling of OMW was carried out during the olive oil extraction period spanning from November 2020 to March 2021. The olive oil extraction units that were chosen are situated in the region of Marrakech-Safi (Morocco), specifically in Al Attaouia city. Samples were taken from the storage pond and transported to the laboratory in large barrels for analysis and processing.

2.2. Experimental tools for block cryoconcentration

Fig. 1 shows a schematic diagram of the principle of treatment of OMW by a combined process of freezing, sweating and thawing (cryoconcentration). First, raw OMW solutions put in 500 mL plastic bottles have undergone cooling and freezing at –24°C to produce an ice block. The refrigerator used is a Robert Bosch Hausgeräte GmbH (81739 München, Germany) (E-Nr (KGN36VL21/17)) with a cooling capacity of 14 kg/24 h. The second step is the sweating or the fractional melting of the ice block at room temperature (about 24°C). It consists of a partial melting of the ice block and its purification in depth by melting the impure zones in pockets of concentrated solutions. The partial melting of the ice block was carried out from the outside of the wall to the inside of the product using the gravitational flow of the concentrated fraction. At the end of this operation, five liquid fractions (F_1, F_2, F_3, F_4, and F_5) were recovered, weighed, and analyzed according to the

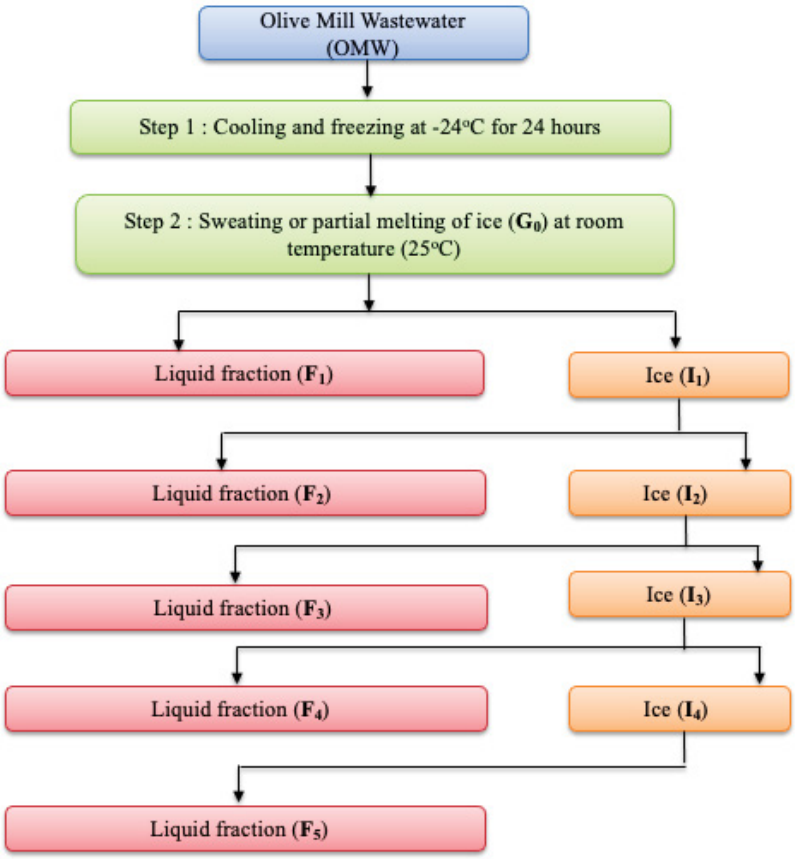

Fig. 1. Treatment of OMW by a combined process of freezing, sweating and thawing (cryoconcentration).

Standard Afnor Methods [39]. The treatment is conducted with five initial solutions of OMW with an initial total dry matter of 10.89%. Five liquid fractions F_1, F_2, F_3, F_4, F_5 were obtained for the five treated solutions (Fig. 2).

Table 1 shows the masses $m_{i=1,2,3,4,5}$ obtained and the recovery times $t_{i=1,2,3,4,5}$ for the five liquid fractions $F_{i=1,2,3,4,5}$ after the sweating step for the five treated solutions. The five cryoconcentrated liquids obtained for the five fractions $F_{i=1,2,3,4,5}$ were collected for analysis.

2.3. Analysis

The pH was measured by a pH meter (model ADWA AD1000). The electrical conductivity (EC in mS/cm at 20°C) was measured by a conductivity meter (WTW inoLab® Cond 730). Suspended matters (SM in g/L) were determined by filtration through 0.45 µm pore size membranes. The SM content is determined from the difference in weight of the filter before and after filtration and drying at 105°C for 12 h. The dry matter content (DM in mass %) was determined after drying at 105°C in an oven for 24 h. The organic matter concentration (OM in mass %) was determined after calcination at 550°C for 12 h. The chemical oxygen demand (COD in g O_2/L) was determined by oxidation with an excess of potassium dichromate in acid medium (H_2SO_4), in the presence of silver sulfate as catalyst and mercury sulfate as chloride complexing agent. The concentration of total phenolic compounds (in g/L) was measured by Folin-Ciocalteu method using a LAMBDA 365 UV/Vis Spectrophotometer (PerkinElmer, USA). The concentration of orthophosphates (PO_4^{3-}) was determined using the spectrophotometric method with ammonium molybdate. The elements Ca, Mg, K, S and Na in OMW samples were analyzed by inductively coupled plasma atomic emission spectroscopy (ICP-AES, iCAP 6000 Series, Thermo Scientific, Cambridge, UK). The UV-Visible scanning spectra of the soluble organic compounds were also recorded. The infrared spectroscopy analysis was performed to identify the chemical functions of the molecules present in the analyzed sample. The spectra were recorded between 4,000 and 550 cm^{-1} using the Thermo Scientific Nicolet iS10 FTIR Spectrometer (Waltham, Massachusetts). Attenuated total reflectance-Fourier-transform infrared spectroscopy analysis was performed on samples dried in a lyophilizer (Alpha 1-2 LDplus Martin Christ).

2.4. Concentration index

The concentration index (CI) was calculated as the ratio between the concentration of the recovered liquid fraction and the concentration of the initial solution [40]:

$$CI = \frac{C_{liq}}{C_0} \quad (1)$$

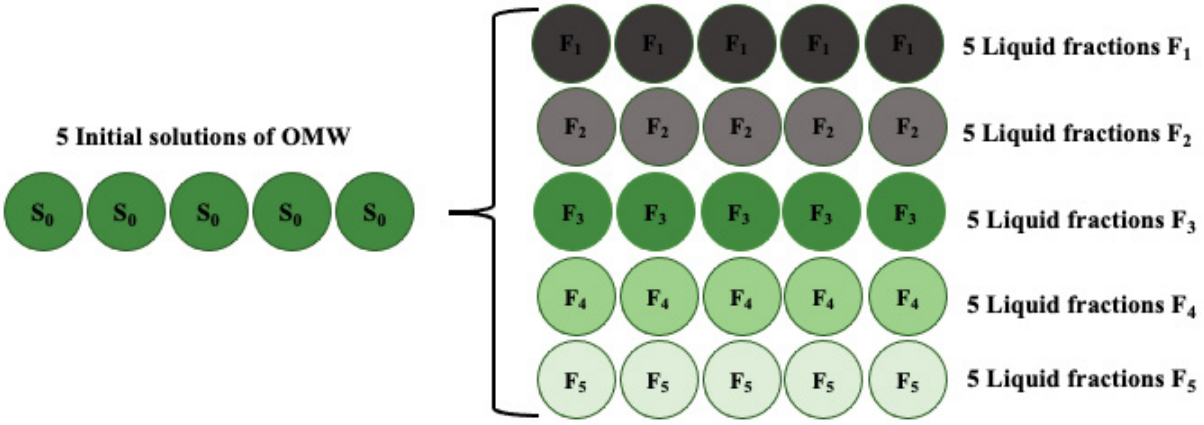

Fig. 2. Initial solutions of raw wastewater and liquid fractions recovered after cryoconcentration treatment.

Table 1
Obtained masses $m_{i=1,2,3,4,5}$ (in g) and recovery times $t_{i=1,2,3,4,5}$ for the five liquid fractions (F_1, F_2, F_3, F_4 and F_5)

S_0	F_1		F_2		F_3		F_4		F_5	
m_T (g)	m_1 (g)	t_1 (min)	m_2 (g)	t_2 (min)	m_3 (g)	t_3 (min)	m_4 (g)	t_4 (min)	m_5 (g)	t_5 (min)
489.80	62.00	84	105.93	154	98.92	232	99.97	313	122.98	–
495.40	60.27	84	94.13	154	99.19	232	76.54	313	165.26	–
506.62	64.07	84	87.48	154	97.88	232	87.97	313	169.21	–
504.29	69.15	84	87.69	154	97.40	232	98.11	313	151.92	–
480.28	66.65	84	96.81	154	107.55	232	94.27	313	115.00	–
Total (g)	322.14	84	472.04	154	500.94	232	456.86	313	724.37	–
Mean (g)	64.43	84	94.41	154	100.18	232	91.37	313	144.87	–

CI was determined for DM, mineral matter (MM), OM, COD and total phenols concentrations. C_{liq} and C_0 are the concentration in liquid fractions obtained after the sweating step and in the initial solution, respectively.

3. Results and discussion

3.1. Analysis of OMW before cryoconcentration treatment

Table 2 shows the physico-chemical characteristics of OMW studied in this work before the cryoconcentration treatment (freezing, sweating and thawing). The results obtained reveal that OMW has an acid pH (pH = 4.55). The acidity of OMW is mainly due to organic acids (phenolic acids and fatty acids). It is also related to their storage time in the ponds [41]. This can be explained by auto-oxidation reactions and polymerization processes that transform phenolic alcohols into phenolic acids [42]. These reactions are manifested by a change in the initial coloration of OMW to a very dark black color [43]. OMW are composed of water (89.98%), organic compounds (7.97%) and mineral compounds (2.92%). Their content of total phenolic compounds is about 28.24 g/L. It also appears that OMW contain phosphate ions (1.15 g/L), potassium (10.39 g/L), calcium (0.88 g/L), sulfur (0.80 g/L), magnesium (0.78 g/L), and sodium (0.64 g/L). The physico-chemical parameters related to the five liquid fractions ($F_{i=1,2,3,4,5}$) will be discussed later in the following paragraphs.

3.2. Evolution of the physico-chemical parameters during OMW cryoconcentration

Figs. 3–5 show the concentrations of DM, MM, OM, COD, total phenols and mineral elements for the liquid fractions $F_{i=1,2,3,4,5}$ obtained after the treatment of OMW by cryoconcentration. The concentration factors for all parameters studied have been presented in Figs. 6 and 7.

The results obtained led to the following findings:

3.2.1. Liquid fraction F_1

The analysis of F_1 fraction highlights an increase in the concentrations of DM, OM and MM which reach respectively the values of 34.28%, 29.01% and 4.29%. These percentages are higher than those obtained in the case of untreated OMW (DM 10.89%, OM 7.97%, MM 2.92%). Likewise, the concentrations of COD and total phenols increased from 230.4 to 768.0 and 28.24 to 100.22 g/L, respectively. The concentration indexes for DM, OM, MM, COD, total phenols, potassium, phosphate, calcium, sulfur, magnesium and sodium are about 3.15, 3.64, 1.47, 3.55, 3.33, 1.78, 1.97, 1.6, 1.3, 1.3 and 1.6, respectively. As

we can seen, there is a good agreement, on the one hand, between the CI of OM and that of COD and total phenols and, on the other hand, between the CI of MM and that of the chemicals elements.

3.2.2. Liquid fraction F_2

In the second cryoconcentrated liquid fraction F_2, the value of DM concentration increased from 10.89% (for the initial solution) to 15.46%. As can be seen, the concentration obtained is 1.42 times higher than that of raw OMW effluent. The concentrations of the organic parameters for the liquid fraction F_2 are higher than those related to the initial OMW. However, the values of the mineral parameters for F_2 are slightly lower than those of the raw wastewater. The concentration factor of OM reaches 1.72. Likewise, this value is consistent with that of COD (1.67) and total phenols (1.90). On the other hand, the concentration index of MM which equals 0.61 is consistent with the CI values for phosphate (0.65), sulfur (0.76), magnesium (0.78), and sodium (0.70) ions. However, the value is lower than that of potassium (1.05) and calcium (1.27).

Table 2
Physico-chemical characteristics of OMW

Parameters	Value
pH	4.55
EC in mS/cm at 25°C	21.68
DM in % at 105°C	10.89
OM in % at 550°C	7.97
MM in % at 550°C	2.92
Density in g/cm^3	0.96
COD in g of O_2/L	230.40
SM in g/L	25.99
Total phenols in g/L	28.24
K^+ in g/L	10.39
PO_4^{3-} in g/L	1.15
Ca^{2+} in g/L	0.88
S^{2-} in g/L	0.80
Mg^{2+} in g/L	0.78
Na^+ in g/L	0.63

3.2.3. Liquid fraction F_3

In the 3rd cryoconcentrated liquid fraction F_3, the amount of DM is 11%. As can be seen, this value is almost identical to the initial DM concentration (10.89%). The organic parameter values for the liquid fraction F_3 are similar to those of the initial solution. The CI of OM which equals 1.19 is consistent with that of COD (1.00) and total phenols (0.86). The CI of the MM decreases to 0.53. As in the case of F_2, this value is consistent with the CI value of phosphate (0.43), sulfur (0.46), magnesium (0.65) and sodium (0.46) ions. However, it is lower than that of potassium (0.86) and calcium (1.09).

3.2.4. Liquid fraction F_4

The concentration of DM in the 4th cryoconcentrated liquid fraction F_4 is 5.93%. It is lower than the initial DM concentration (10.89%). The values of the organic parameters and minerals for the liquid fraction F_4 are also lower than those related to the initial solution. The CI of the OM which reaches 0.54 is consistent with the CI of COD (0.67) and total phenols (0.26). The CI for MM which is of the order of 0.25 is in agreement with that of potassium (0.20), phosphate (0.24), calcium (0.3), sulfur (0.33), magnesium (0.15) and sodium (0.37) ions.

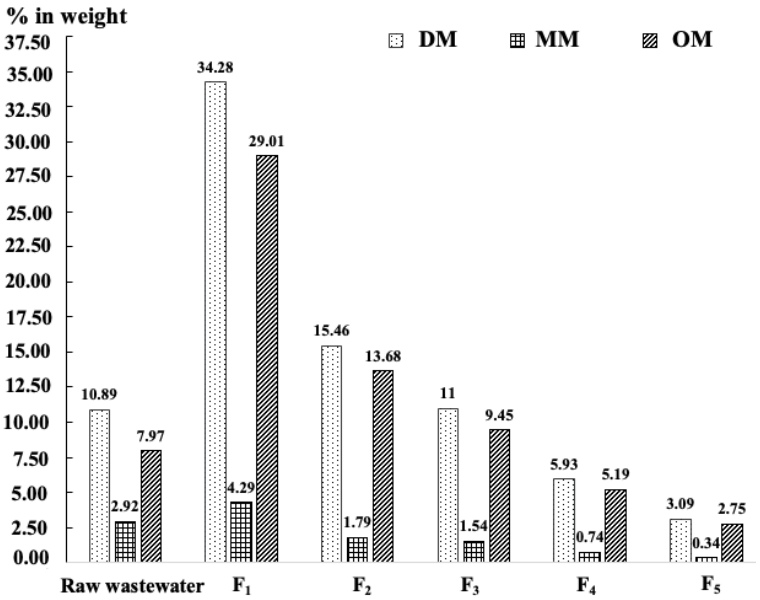

Fig. 3. Concentrations of DM, MM and OM for the raw OMW and the liquid fractions $F_{i=1,2,3,4,5}$ obtained after the cryoconcentration treatment (freezing, sweating and thawing).

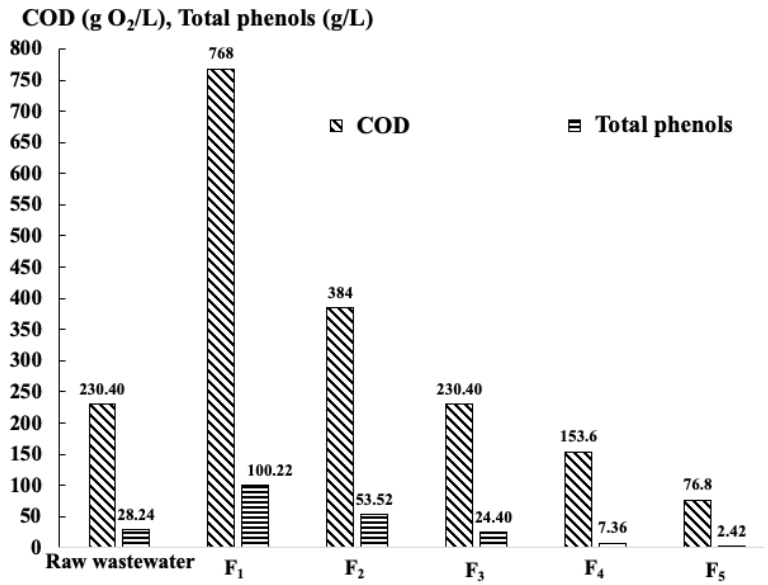

Fig. 4. COD and total phenols concentrations for the raw OMW and the liquid fractions $F_{i\,=\,1,2,3,4,5}$ obtained after the cryoconcentration treatment (freezing, sweating and thawing).

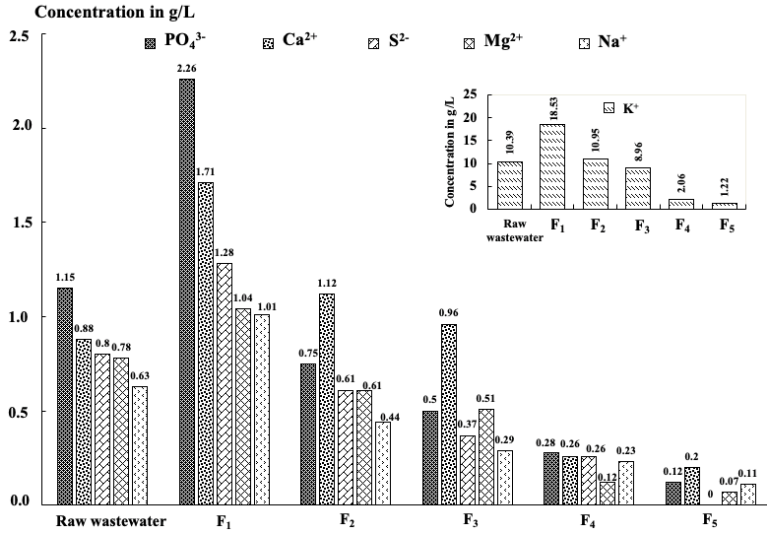

Fig. 5. Concentration of PO_4^{3-}, Ca^{2+}, S^{2-}, Mg^{2+}, Na^+ and K^+ for the raw OMW and the liquid fractions $F_{i\,=\,1,2,3,4,5}$ obtained after the cryoconcentration treatment (freezing, sweating and thawing).

3.2.5. Liquid fraction F_5

In the last cryoconcentrated liquid fraction F_5, the concentration of DM is reduced to 3.09%. It is much lower than that of the raw OMW. The values corresponding to the organic and mineral parameters for F_5 are also much lower than those related to the initial wastewater. The CI of the OM decreased to the value 0.35 which is consistent with that of COD (0.34) and total phenols (0.09). The CI for MM which is about 0.12 reflects that of K^+, PO_4^{3-}, Ca^{2+}, S^{2-}, Mg^{2+} and Na^+.

All of these results can be discussed and interpreted as follows:

The cooling and freezing step of the treated solutions are performed in static mode; freezing is usually conducted by applying a constant temperature of about –24°C in the refrigerator cold room. A more or less significant thermal gradient is thus imposed between the outer surface of the bottle and it's interior. This produces a concentration gradient within the solution by the rejection of salt during the rapid ice growth. The temperature at the ice/solution interface tends to increase due to the release of heat produced by freezing, following the increase in concentration which results in a decrease in the freezing temperature and, finally, because of the high thermal resistance of the solid.

During the step of freezing, the growing ice rejects solutes (organic and mineral) towards the solution and concentration gradients also appear in the solution, especially if the growth is rapid. The highly concentrated solution at the ice/solution interface is, thereby, denser than the solution outside the flask.

The effect of the thermal gradient applied across the solution can be explained by the morphological instability phenomenon at the ice/solution interface. However, it can also be explained by the incorporation of pockets of solutions concentrated in solutes (organic and mineral matter) in the ice block. The solutes contained in the ice block formed during the crystallization step are in the form of solution pockets [28,31,33]. Their concentration is likely to be higher than the concentration of the initial solution, since the solution is concentrated during the freezing step. Some scenarios can be suggested to explain the different mechanisms for the incorporation of the solution pockets in the ice. First, the presence of dissolved gases in the medium can explain the incorporation of solute. On the other hand, the mechanism of adsorption of organic molecules on ice has already been highlighted in the literature. Microstructure analysis of the freezing of acetone solutions identified mechanisms of impurity incorporation into the ice. Other factors may be at the origin of these incorporations, one of which is the adsorption of organic solute and the presence of dissolved gas at the surface of the ice layer [44].

During the sweating step, the ice block is subjected to room temperature. The temperature of the ice block is increased, causing a thermal gradient in the crystalline layer; this will partially remelt the areas or channels containing the solutes. These, under the effect of gravity, flow along the crystalline layer; the process is therefore driven by heat transfer. During this step, the sudden ice cracks, allowing bridges between these pockets of concentrated solutions to be formed. This further allows the evacuation of the solution to the outside. The concentrated solution is mainly trapped in the interstices between the ice crystals. The network formed by the grain boundaries offers privileged conditions for the drainage of the concentrated solution under the influence of gravity. The visual aspect of the ice obtained in the last fraction shows a very fragile ice for the most concentrated solutions and hard ice for the less concentrated solutions. High concentration ice is porous and dendritic, while low concentration ice is more compact. The monitoring of the visual aspect of these ice blocks during the penetrant stage, showed a strongly cracked ice for all the studied solutions. These cracks explain why it is possible to purify the layer in depth. The highly concentrated solutions were the first and second liquid fractions F_1 and F_2. The liquid fraction F_3 is less concentrated and its concentration is relatively equal to that of the initial solution (untreated OMW). Finally, the most dilute liquid fractions were F_4 and F_5. As a result, further studies of these complex phenomena related to thermal and material transfers are necessary. These tests made it possible to identify the operating conditions to be implemented in a process of treatment of OMW by cryoconcentration in block. The test will also identify the key operating parameters that affect the concentration increase reached in the first liquid fraction F_1 and the purity of the ice obtained in the last liquid fraction F_5. These parameters are the cooling and freezing temperature, the concentration of the initial OMW solution and the number of liquid fraction obtained after the partial melting of the ice block. A systematic study of the effect of these operating parameters is necessary.

3.3. UV-Visible analysis

Fig. 8 shows the UV-Visible spectra for the cryoconcentrated liquid fractions $F_{i\,=\,1,2,3,4,5}$ obtained after treatment of OMW effluent. The broad band observed around 278 nm is a characteristic of phenols [45]. The studied OMW

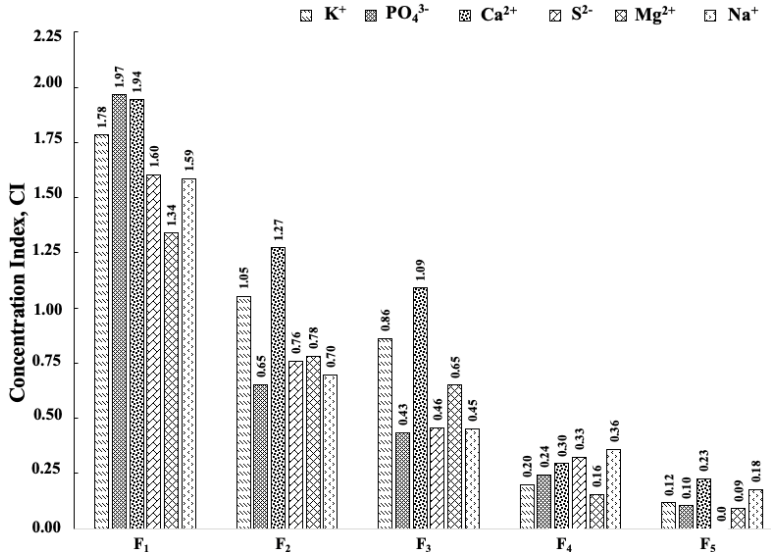

Fig. 6. Concentration index (CI) of mineral elements for the liquid fractions $F_{i\,=\,1,2,3,4,5}$ obtained after the cryoconcentration treatment (freezing, sweating and thawing).

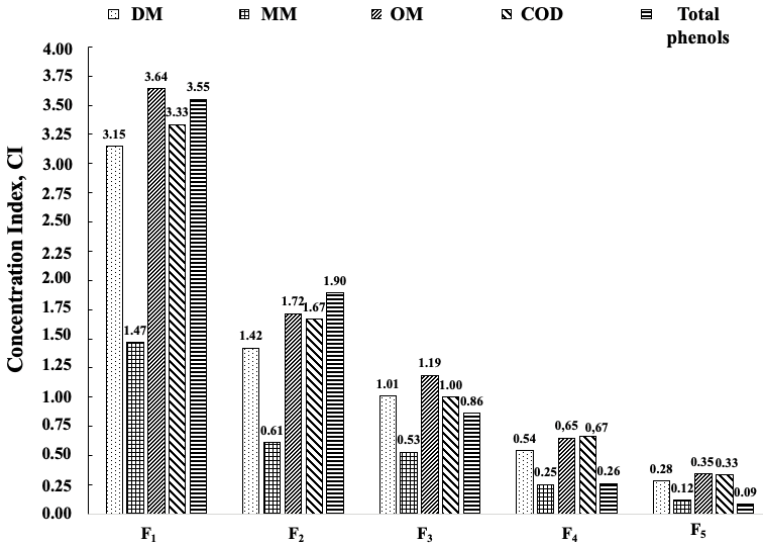

Fig. 7. Concentration index (CI) of the physico-chemical parameters for the liquid fractions $F_{i\ =\ 1,2,3,4,5}$ obtained after the cryoconcentration treatment (freezing, sweating and thawing).

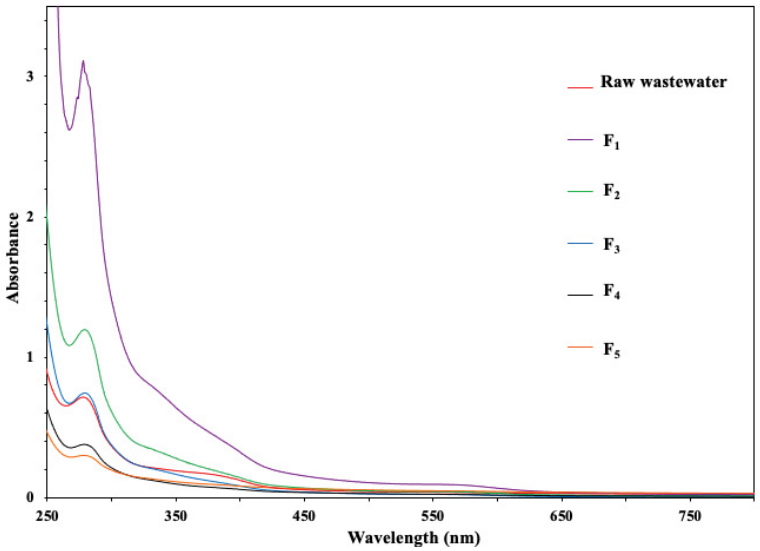

Fig. 8. UV-Visible spectra for the liquid fractions $F_{i\ =\ 1,2,3,4,5}$ obtained after the treatment of OMW by cryoconcentration (freezing, sweating and thawing).

solutions have a brown coloration which would be related to phenolic compounds. The reduction in absorption intensity at 278 nm is mainly due to the decrease in the quantity of OM, especially polyphenols. The most concentrated solution is F_1, however the absorbance of liquid fraction F_5 is very low compared to that of raw OMW. This is due to the decrease of OM amount in the last liquid fraction obtained. These results are consistent with the quantitative analysis obtained by the Folin-Ciocalteu method.

3.4. FTIR analysis

Fig. 9 shows the infrared spectra for the $F_{i\ =\ 1,2,3,4,5}$ fractions obtained after treatment of OMW. Samples analyzed were first dried in a lyophilizer. The assignment of the bands to the functional groups characteristic of OMW and cryoconcentrated liquid fractions is carried out on the basis of the research work in the literature [46–48]. Indeed, the broad band centered at 3,290 cm^{-1} is due to the elongation vibrations of the free O–H bonds of phenolic compounds and alcoholic compounds and to N–H elongation vibrations of primary and secondary amides and amines. The bands located at 2,929 and 2,876 cm^{-1} are due to the elongation vibrations of the methyl and methylene groups, respectively. The band noted at 1,715 cm^{-1} is mainly due to the C=O elongation vibrations of the carboxylic acids. The transmission intensity recorded at 1,582 cm^{-1} is the result of the C=C elongation vibration of aromatic

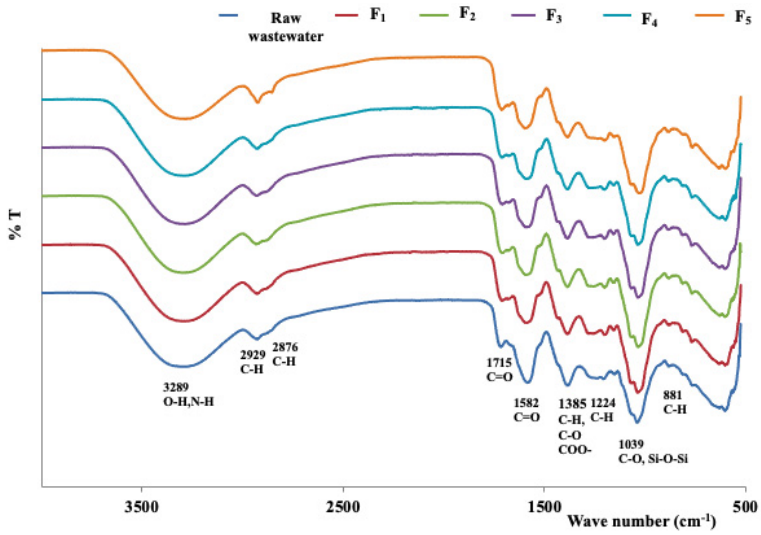

Fig. 9. Attenuated total reflectance-Fourier-transform infrared spectra of the liquid fractions $F_{i\ =\ 1,2,3,4,5}$ obtained after the treatment of OMW by cryoconcentration (freezing, sweating and thawing).

compounds and the N–H deformation of secondary amines and amides. The band at 1,385 cm^{-1} was assigned to O–H and C–O of the phenolic moiety, COO^-, and C–H of methylene. The band centered at about 1,420 cm^{-1} is commonly attributed to C=O and C=C elongation vibrations of aromatic compounds. The weak bands centered at 1,210 and 1,320 cm^{-1} respectively indicate the presence of the O-H group of phenolic compounds [49]. The weak bands centered at 1,350 and 1,250 cm^{-1} are commonly attributed to the presence of the CH_2 group in cyclic molecules and thus to the elongation of the C–O bonds of phenolic compounds and organic acids. The intense band observed at 1,039 cm^{-1} is often attributed to the C–O groups of polysaccharides and to the inorganic fraction of the sample. The typical peak at 881 cm^{-1} can be attributed to the deformation of the C–H group of aromatic compounds and the presence of some minerals such as carbonates and silica.

4. Conclusion

The experiments carried out make it possible to identify the operating conditions to be implemented in a process for treating OMW by freezing and thawing. The treatment produced five cryoconcentrated liquid fractions (F_1, F_2, F_3, F_4 and F_5). The results show that the liquid fraction F_1 is characterized by a CI equals 3.6 and 1.5 for organic parameters (OM, COD, and total phenols) and mineral matter, respectively. This fraction is characterized by a maximum concentration of phenolic compounds (about 100.22 g/L). The cryoconcentrated liquid fraction F_2 has a CI equals 1.7 and 0.6 for OM and MM, respectively. The CI for the liquid fraction F_3 is approximately between 1.2 and 0.5. This liquid has physico-chemical characteristics similar to those of raw OMW. The CI corresponding to the 4th and 5th fractions decreased to values 0.65–0.35 and 0.25–0.12 in terms of organic and mineral matter, respectively. The characterization of the last liquid fraction F_5 produced shows a significant reduction in OM and MM contents. The experiments showed that the sweating step allowed a deep purification of the ice layer. The concentration factor of OM in the obtained F_5 liquid fraction decreased to 0.35. These values are consistent with the decrease in COD and total phenols concentrations. The CI for MM which is reduced to 0.12 is consistent with the decrease in the concentrations of potassium, phosphate, calcium, sulfur, magnesium and sodium.

Generally, the experimental results show the feasibility and importance of the cryoconcentration process to produce cryoconcentrated solutions of total phenolic compounds. The study of the influence of the operating parameters such as initial DM concentration, cooling temperature and number of liquid fractions applied during the sweating step is in progress. The valorization of phenolic compounds from cryoconcentrated OMW is also one of our ongoing research interests.

References

[1] A. El-Abbassi, H. Kiai, A. Hafidi, Phenolic profile and antioxidant activities of olive mill wastewater, Food Chem., 132 (2012) 406–412.
[2] S. Dermeche, M. Nadour, C. Larroche, F. Moulti-Mati, P. Michaud, Olive mill wastes: biochemical characterizations and valorization strategies, Process Biochem., 48 (2013) 1532–1552.
[3] R. Cossu, N. Blakey, P. Cannas, Influence of codisposal of municipal solid waste and olive vegetation water on the anaerobic digestion of a sanitary landfill, Water Sci. Technol., 27 (1993) 261–271.
[4] M. Jusoh, R. Mohd. Yunus, M.A. Abu Hassan, Development of a New Crystallisation Chamber for a Progressive Freeze Concentration System, M.A. Strangio, Ed., Recent Advances in Technologies (Chapter 33), InTechOpen Europe, ISBN 978-953-307-017-9, 2009, pp. 587–599.
[5] N. Meksi, W. Haddar, S. Hammami, M.F. Mhenni, Olive mill wastewater: a potential source of natural dyes for textile dyeing, Ind. Crops Prod., 40 (2012) 103–109.
[6] T. Yangui, S. Sayadi, A. Rhouma, A. Dhouib, Potential use of hydroxytyrosol-rich extract from olive mill wastewater as a biological fungicide against *Botrytis cinerea* in tomato, J. Pest Sci., 83 (2010) 437–445.

[7] B. Mechri, H. Chehab, F. Attia, F.B. Mariem, M. Braham, M. Hammami, Olive mill wastewater effects on the microbial communities as studied in the field of olive trees by analysis of fatty acid signatures, Eur. J. Soil Biol., 46 (2010) 312–318.
[8] N.A. Oz, A.C. Uzun, Ultrasound pretreatment for enhanced biogas production from olive mill wastewater, Ultrason. Sonochem., 22 (2015) 565–572.
[9] I. Aviani, Y. Laor, S. Medina, A. Krassnovsky, M. Raviv, Co-composting of solid and liquid olive mill wastes: management aspects and the horticultural value of the resulting composts, Bioresour. Technol., 101 (2010) 6699–6706.
[10] K. Gerasopoulos, D. Stagos, S. Kokkas, K. Petrotos, D. Kantas, P. Goulas, D. Kouretas, Feed supplemented with byproducts from olive oil mill wastewater processing increases antioxidant capacity in broiler chickens, Food Chem. Toxicol., 82 (2015) 42–49.
[11] F.J. Rivas, F.J. Beltrán, O. Gimeno, J. Frades, Treatment of olive oil mill wastewater by Fenton's reagent, J. Agric. Food Chem., 49 (2001) 1873–1880.
[12] M.S. Fountoulakis, S.N. Dokianakis, M.E. Kornaros, G.G. Aggelis, G. Lyberatos, Removal of phenolics in olive mill wastewaters using the white-rot fungus *Pleurotus ostreatus*, Water Res., 36(2002) 4735–4744.
[13] M. Drouiche, V. Le Mignot, H. Lounici, D. Belhocine, H. Grib, A. Pauss, N. Mameri, A compact process for the treatment of olive mill wastewater by combining OF and UV/H_2O_2 techniques, Desalination, 169 (2004) 81–88.
[14] H. El Hajjouji, N. Fakharedine, G. Ait Baddi, P. Winterton, J.R. Bailly, J.C. Revel, M. Hafidi, Treatment of olive mill wastewater by aerobic biodegradation: an analytical study using gel permeation chromatography, ultraviolet–visible and Fourier transform infrared spectroscopy, Bioresour. Technol., 98 (2007) 3513–3520.
[15] J.M. Ochando-Pulido, M. Stoller, L. Di Palma, A. Martinez-Ferez, Threshold performance of a spiral-wound reverse osmosis membrane in the treatment of olive mill effluents from two-phase and three-phase extraction processes, Chem. Eng. Process. Process Intensif., 83 (2014) 64–70.
[16] A. Zyoud, H. Nassar, A. El-Hamouz, H.S. Hilal, Solid olive waste in environmental cleanup: enhanced nitrite ion removal by $ZnCl_2$-activated carbon, J. Environ. Manage., 152 (2015) 27–35.
[17] M. Jeguirim, P. Dutournié, A.A. Zorpas, L. Limousy, Olive mill wastewater: from a pollutant to green fuels, agricultural water source and bio-fertilizer—part 1. The drying kinetics, Energies, 10 (2017) 1423, doi: 10.3390/en10091423.
[18] R. Zakia, E.H. Mounia, B. Mohammed, M. Zineb, L. Kenza, T. Mustapha, Z. Youness, R. Rabie, B. Hassan, N. Mostafa, Olive mill wastewater: treatment, valorization in the germination of tomato seeds and in the composting, J. Water Sci., 30 (2017) 57–62.
[19] F. Elayadi, W. Boumya, M. Achak, Y. Chhiti, F.E.M. Alaoui, N. Barka, C.E. Adlouni, Experimental and modeling studies of the removal of phenolic compounds from olive mill wastewater by adsorption on sugarcane bagasse, Environ. Challenges, 4 (2021) 100184, doi: 10.1016/j.envc.2021.100184.
[20] G. Tanguy, A. Dolivet, S. Méjean, D. Garreau, F. Talamo, P. Postet, R. Jeantet, P. Schuck, Efficient process for the production of permeate powders, Innovative Food Sci. Emerg. Technol., 41 (2017) 144–149.
[21] S. Okawa, T. Ito, A. Saito, Effect of crystal orientation on freeze concentration of solutions, Int. J. Refrig., 32 (2009) 246–252.
[22] A.L. Zydney, Membrane handbook edited by W.S. Winston Ho, and Kamalesh K. Sirkar, Van Nostrand Reinhold, New York, 1992, AIChE J., 41 (1995) 2343–2344.
[23] A. Rich, Y. Mandri, Dessalement des eaux marines et saumâtres par congélation: Aspects thermodynamiques, cinétiques, paramétrique, thermique et énergétique, Éditions Universitaires Européennes, ISBN: 978-3-639-62264-5, 2017, 240 Pages.
[24] Y. Mandri, A. Rich, D. Mangin, A. Rivoire, C. Bebon, J.P. Klein, T. Bounahmidi, A. et Bouhaouss, C. Cogné, Dessalement de L'eau de Mer Par Congélation, Revue Générale du Froid et du Conditionnement d'Air, N°1133, 2013, pp. 58–69.
[25] F. Melak, A. Ambelu, G.D. Laing, E. Alemayehu, Freeze desalination as point of use water treatment technology: a case of chromium(VI) removal from water, Proceedings, 2 (2018) 173, doi: 10.3390/ecws-2-04942.
[26] A. Najim, A review of advances in freeze desalination and future prospects, npj Clean Water, 5 (2022), doi: 10.1038/s41545-022-00158-1.
[27] P. Orellana-Palma, G. Petzold, M. Guerra-Valle, M. Astudillo-Lagos, Impact of block cryoconcentration on polyphenol retention in blueberry juice, Food Biosci., 20 (2017) 149–158.
[28] M. Guessous, A. Rich, S. Mountadar, F.Z. Karmil, J. El Hajri, M. Mountadar, M. Siniti, Experimental study of wastewater treatment containing sulfuric acid solutions using freezing and thawing method, Desal. Water Treat., 211 (2021) 141–152.
[29] S. Samsuri, N.A. Amran, N. Yahya, M. Jusoh, Review on progressive freeze concentration designs, Chem. Eng. Commun., 203 (2016) 345–363.
[30] A. Rich Y. Mandri, N. Bendaoud, D. Mangin, S. Abderafi, C. Bebon, N. Semlali, J.-P. Klein, T. Bounahmidi, A. Bouhaouss, S. Veesler, Freezing desalination of sea water in a static layer crystallizer, Desal. Water Treat., 13 (2010) 120–127.
[31] A. Rich, Y. Mandri, D. Mangin, A. Rivoire, S. Abderafi, C. Bebon, N. Semlali, J.-P. Klein, T. Bounahmidi, A. Bouhaouss, S. Veesler, Sea water desalination by dynamic layer melt crystallization: parametric study of the freezing and sweating steps, J. Cryst. Growth, 342 (2012) 110–116.
[32] M. Rich, D. Siniti, D. Mangin, J.-P. Klein, Y. Mandri, T. Bounahmidi, A. Bouhaouss, S. Veesler, M. El Ganaoui, Study of a melt crystallization process for seawater desalination, J. Mech. Eng. Autom., 5 (2015) 45–52.
[33] Y. Mandri, A. Rich, D. Mangin, S. Abderafi, C. Bebon, N. Semlali, J.-P. Klein, T. Bounahmidi, A. Bouhaouss, Parametric study of the sweating step in the seawater desalination process by indirect freezing, Desalination, 269 (2011) 142–147.
[34] E. Hernández, A. Santos, N. Pazmiño, M. Raventós, M. Blanco, F.L. Moreno, Y. Ruiz, A. Rich, S. Samsuri, Two strategies for freeze desalination of seawater by progressive and block techniques, Desal. Water Treat., 215 (2021) 1–9.
[35] A. Balde, M. Aïder, Effect of cryoconcentration, reverse osmosis and vacuum evaporation as concentration step of skim milk prior to drying on the powder properties, Powder Technol., 319 (2017) 463–471.
[36] P. Guillermo, O. Patricio, M. Jorge, V. Prisila, Physico-chemical properties of cryoconcentrated orange juice, Chem. Eng. Trans., 75 (2019) 37–42.
[37] S. Mountadar, M. Guessous, A. Rich, F.Z. Karmil, H. El Alaoui Belghiti, M. Siniti, S. Tahiri, Desalination of spent ion-exchange resin regeneration solutions by suspension freeze crystallization, Desalination, 468 (2019) 114059, doi: 10.1016/j.desal.2019.06.025.
[38] T. Htira, C. Cogné, G. Gagnière, D. Mangin, Experimental study of industrial wastewater treatment by freezing, J. Water Process Eng., 23 (2018) 292–298.
[39] AFNOR, French Association for Standardization, Collection of Standards, Water, Essay Methods, Edition 1987, 1989.
[40] F.L. Moreno, E. Hernández, M. Raventós, C. Robles, Y. Ruiz, A process to concentrate coffee extract by the integration of falling film and block freeze-concentration, J. Food Eng., 128 (2014) 88–95.
[41] L. Chaari, N. Elloumi, S. Mseddi, K. Gargouri, B.B. Rouina, T. Mechichi, M. Kallel, Changes in soil macronutrients after a long-term application of olive mill wastewater, J. Agric. Chem. Environ., 4 (2015) 1–13.
[42] M. Hamdi, J.L. Garcia, Comparison between anaerobic filter and anaerobic contact process for fermented olive mill wastewaters. Bioresour. Technol., 38 (1991) 23–29.
[43] N. Assas, L. Ayed, L. Marouani, M. Hamdi, Decolorization of fresh and stored-black olive mill wastewaters by *Geotrichum candidum*, Process Biochem., 38 (2002) 361–365.
[44] T. Htira, C. Cogné, E. Gagnière, D. Mangin, Determination of the solid–liquid phase diagram of the binary system propionic acid/water, J. Chem. Eng. Data, 61 (2016) 806–812.

[45] M. Hamdi, J.L. Garcia, R. Ellouz, Integrated biological process for olive mill wastewater treatment, Bioprocess Eng., 8 (1992) 79–84.
[46] J.S. Ribeiro, S.S. Ok, S. Garrigues, M. de la Guardia, FTIR tentative characterization of humic acids extracted from organic materials, Spectrosc. Lett. Int. J. Rapid Commun., 34 (2001) 179–190.
[47] G. Ait Baddi, J.A. Alburquerque, J. Gonzálvez, J. Cegarra, M. Hafidi, Chemical and spectroscopic analyses of organic matter transformations during composting of olive mill wastes, Int. Biodeterior. Biodegrad., 54 (2004) 39–44.
[48] C. Peltre, S. Bruun, C. Du, I.K. Thomsen, L.S. Jensen, Assessing soil constituents and labile soil organic carbon by mid-infrared photoacoustic spectroscopy, Soil Biol. Biochem., 77 (2014) 41–50.
[49] J. Hejzlar, B. Szpakowska, R.L. Wershaw, Comparison of humic substances isolated from peatbog water by sorption on DEAE-cellulose and amberlite XAD-2, Water Res., 28 (1994) 1961–1970.